Proc. of the 6th Intl. Symposium on Reliability Engineering and Risk Management (6ISRERM)
31 May – 1 June 2018, Singapore
Editor(s) Xudong Qian, Sze Dai Pang, Ghim Ping Raymond Ong, Kok-Kwang Phoon

ARCHING EFFECT ON GEO-SYNTHETIC REINFORCED PILE-SUPPORTED EMBANKMENT SUBJECTED TO CYCLIC LOADING: NUMERICAL STUDY

ZHANG ZHEN[1], TAO FENGJUAN[1], YE GUANBAO[1] and LIU LIU[1]

[1]*Department of Geotechnical Engineering, Tongji University, Shanghai, China.*
E-mail: secondauthor_662taofengjuan@tongji.edu.cn

Geosynthetic-reinforced pile-supported embankments, as an economic and effect construction technique to reduce total and differential settlements and enhance load transfer efficiency for embankments, have been widely used in soft soils. Most studies have been done so far to investigate this embankment system under static loads. However, highway and railway embankments are subjected to cyclic loading. The behavior of this embankment system under cyclic loading is not well known, therefore, it deserves further research. In this study, based on a scale test, the fainant element method (FE model) incorporated in the 3D was adopted. A local cyclic load was applied on the top of the model and the deformation and pressure on the load-transfer platform and the tension in the geogrid under cyclic loading were monitored and analyzed. The numerical analysis shows that the cyclic load increased the differential settlement and miner the arching effect under cyclic loading and the lower load frequency has higher damage of arching effect.

Keywords: Pile-supported embankment, Cyclic load, Soil arching, FE model.

1 Introduction

Geosynthetic-reinforced pile-supported embankments has been widely used to geotechnical engineering (Jones 1990, Low et al. 1994; Russell et al., 1997) for providing an economic and effective solution to enhance the bearing capacity and stability and carry small total and differential settlements compared to the traditional foundation treatment methods. As for this method, the loads due to the embankment are transmitted to the piles either directly by arching effect in the embankment soil, or indirectly through the way of membrane effect in the geosynthetic reinforcement (Terzaghi 1943, Villard 2004).

Most of the previous studies was mainly account for the surcharge load by introducing a vertical, uniformly distributed static load (BSI 2010, EBGEO 2010). However, after putting in use railway and highway constructed with piled embankments, the soil arching existing in piled embankments will probably carry on cyclic traffic loadings. And then, the features of soil arching in this condition will be influenced. Heitz point out through model test (Heitz, 2008) that cyclic-dynamic loads lead to a changed load-transfer mechanism, as a reformed arching effect in the bearing. Han jie et al. (Han 2009) compared the arching behavior of the unreinforced embankment and the geogrid-reinforced pile-supported embankment and found that the geosynthetic reinforcement can improve the the stress concentration ratio and decrease the deformation of embankment under cyclic load. The current researches about the behavior of this embankment system under cyclic loading were still not well known, therefore, it deserves further research.

The soil arching behavior in the geosynthetic reinforced pile-supported embankment under cyclic loading is studied in this thesis by means of numerical analysis model which is based on a scale test finished by Van Eekelen et al. (Eekelen 2012I,II). Then, the influences of cyclic load to the arching once formulated after fill construction and the parameter studys of the load frequency (f) were investigated. Load frequency 0 Hz (static load) is take into account to make a comparison. A local load area is used to take place the unit load to better model the real condition of traffic load.

2 Numerical modeling

Eekelen (Eekelen 2012I, II) performed a series of twelve 3D laboratory model tests on piled embankment and the tests were conducted using the test set-up shown in Figure 1. In this paper, only the K2 test was considered. Test setup details refer to the literature (Eekelen 2012I, II). Based on the test, a 3-dimentional finite element (FE) model, with the same model size as scale test, is created using ABAQUS 6.14. Table 1. tabulate the material properties used in the FE model. Most properties of subsoil were obtained from the scale test.

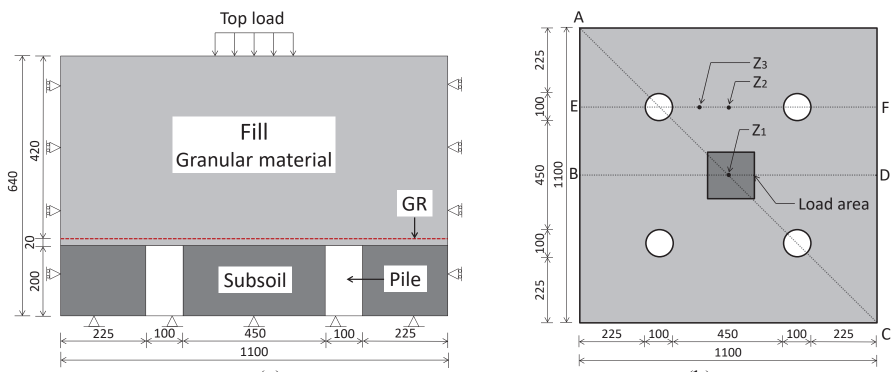

Figure 1. Side view and top view of model set-up (Unit: mm).

Table 1. Material properties

Material	Model	E (KPa)	EA (kN/m)	γ (kN/m^3)	μ	φ (°)	Ψ (°)	c (kPa)
Pile	Elastic	1000000	-	13.60	0.10	-		-
Subsoil	Elastic	17	-	10.20	0.35	-		-
GR	Elastic	-	2269	-	0.10	-		-
Fill	M-C	31000	-	16.58	0.20	49	19	0.5

Note: E = Young's modulus; EA= Stiffness GR J2% ; γ = unit weight; μ = Poisson's ratio; φ = a peak friction angle; Ψ = a dilatation angle; c = cohesion

In the scale test, each top load step is followed by a consolidation steps, after which, the system was allowed to stabilize for a enough long time until the measurements became stable. For the FE simulation, every load step was simplified as a complete drainage process, so that, the drained soil properties were applied to the subsoil was not considered. The friction between the wall of the metal model box and the granular material is calculated as about 20% of the whole top load (Eekelen 2013). To keep the amount of load distribution comparable to the scale test, the top load is reduced to 80% in the FE model (from 0-25-50-75-100kPa reduced to 0-20-40-60-80kPa).

In this paper, based on the above FE model, the soil arching under cyclic loading was investigated. The cyclic load in this paper was modeled using a simple cosine curve which could be shown in Figure 2. A localized loading with an area of 0.22m×0.22m (shown in Figure 1(b)) was used to better model the real condition of traffic load. Different frequency 0.1 Hz; 1 Hz; 10 Hz of cyclic load was taken into consideration and a static load with frequency of 0 Hz was used as a contrast. The number of cyclic load in this analysis is taken as 200 cycles, until the measurements became stable in all frequency. The time-history curve of the cyclic load (0.1 Hz) within two cycles was shown in Figure 2.

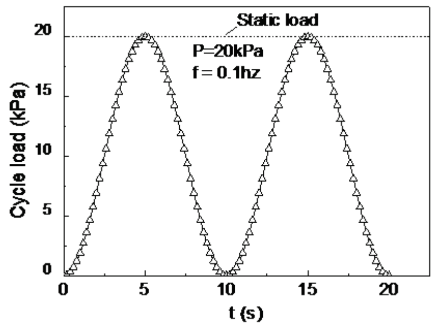

Figure 2. Time–history curve of the cyclic loading of which frequency is 0.1 Hz.

3 Model validations

Displacements at Z_1 and Z_3 of the FE model are shown in Figure 3(a). It can be seen that the displacements of numerical model agreed well with the test data. But the numerical displacements were a bit higher than the test when the top load is zero. This might because that the friction of wall and granular reduced the displacement caused by fill gravity in scale test which is not exist in FE model. Besides, as Figure 3(b) shown, the load transferred directly to the piles due to arching (load part A) and the load transferred through the geosynthetic reinforcement to the piles (load part B) both increased with applied load as the same as scale test. During the filling step and the first two step of top load, the numerical results of load parts A and B agree quite well with the test results. However, after that, the numerical results begin to diverge from the test results that load part A is overestimated and load part B is underestimated. At the same time, the numerical load parts A% and B% show a smooth relationship with the top load which seems somewhat differ from the conclusion of the test that load parts A% decreased while load parts B% increased.

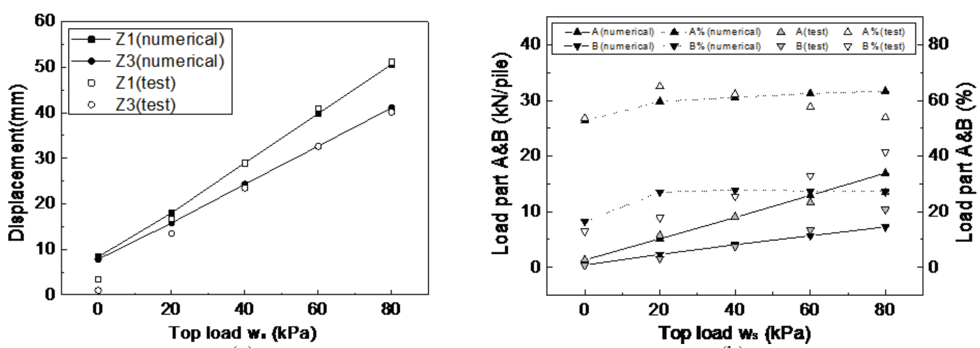

(a) (b)

Figure 3. Variation of vertical deflection and load distribution: (a)vertical deflection; (b) load distribution both in kN/pile and as a % of total load A + B + C.

4 Results and discussion

4.1 *Differential settlement*

Figure 4 shows the settlement distribution on footing of embankment under 200 load cycles with different frequency. Due to the symmetry of the structure, only a quarter of the embankment was shown. There was almost no settlement of embankment above the pile cap. While, it increased very much at the edge of pile cap and reached a balance value over the middle of subsoil. The settlement over the subsoil near model boundary (side A&B) was always smaller than that near the middle of four piles. Because, the load area was limited in the middle of four piles, so that it would have small effects to the other scope. Besides, it is noteworthy to mention that the settlement of the embankment under the load with low-frequency 0.1 Hz was almost as the same as 1 Hz and was very close to static load. While, the settlement under the load with frequency of 10 Hz was much larger than static load. Regardless of frequency of the load, the biggest differential settlement was happened in the middle of four piles (Z_1).

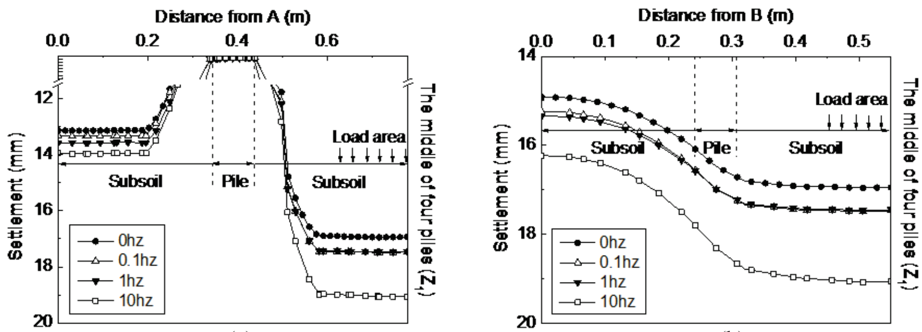

Figure 4. Settlement distribution on footing of embankment: (a)line AC; (b)line BD.

Figure 5 shows that the displacement caused by cyclic load in Z1 increased with the load cycles, which can be attributed to the accumulation of plastic strain under the cyclic load. Just like Figure 5 shows, the displacements of 0.1 Hz and 1 Hz in the whole process of load cycling always had a similar regulation. Moreover, the displacements under cyclical load of lower frequency 0.1 Hz and 1 Hz increasing faster than the higher one and stabilize earlier, but, the stable deformation it reached is much smaller than 10 Hz after 200 cycles. The displacement corresponding to those three frequency 0.1 Hz; 1 Hz and 10 Hz is 8.03mm; 8.00mm and 9.70mm. According to the comparison, the displacement under static load 7.50mm is approximately 23% smaller than that of the cyclic load of 10 Hz and 6% of 0.1 Hz and 1 Hz.

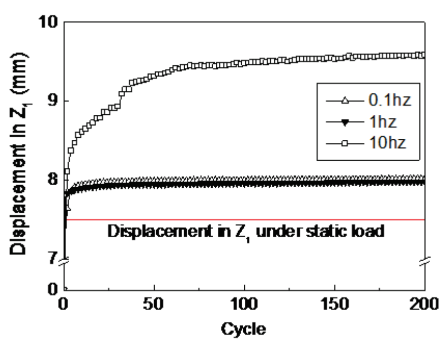

Figure 5. Displacement caused by top load at Z1 versus load cycles.

4.2 *Earth pressure at base of load-transfer platform*

The earth pressure of the embankment at base of load-transfer platform can be divided to load part A; load part B and load part C, defined respectively as the part of the load directly transmitted by the soil arch to the pile; the part of the load transmitted by the geosynthetic reinforcement (GR) to the pile and the part of the load supported by the subsoil. Figure 6 shows the load part A and B as a percentage of the total load A+B+C at base of load-transfer platform (A% and B%). Under the cyclic load, the variation of load part A% was almost with the same regulation at different frequency that A% decreased rapidly and then tend to be stable with the load cycles. Load part A% after 200 cycles of 10 Hz is slightly higher than those of 0.1 Hz and 1Hz, and they are about 12~17% smaller than those without top load. However, the load part B% displays a contrary law with A% that the higher the frequency, the more the load part B% decreases and there result has a quit difference that 10 Hz is approximately 21% lower than 0.1 Hz and 1 Hz and 31% lower than those without top load.

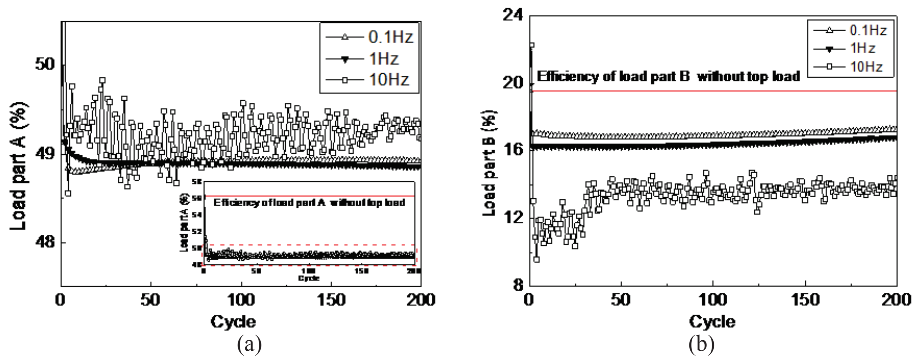

Figure 6. Efficiency of load part A&B of total load versus load cycles: (a) Load part A, (b) Load part B.

4.3 *Tensile stress in geo-synthetics*

The tensile stresses in geo-synthetics alone line AC and EF with different load frequency is shown in Figure 7. The tensile stress under cyclic load is much higher than those without top load especially of the maximum stress. The maximum stresses after cyclic loading are 109kpa alone line AC and 118kpa alone EF which are respectively 62% and 66% larger than those before loading. Moreover, the tensile stress under cyclic load of 10 Hz is a somewhat lower than of 0.1 Hz and 1 Hz at the areas of the cyclic load alone line AC in Figure 7(a) and of the top

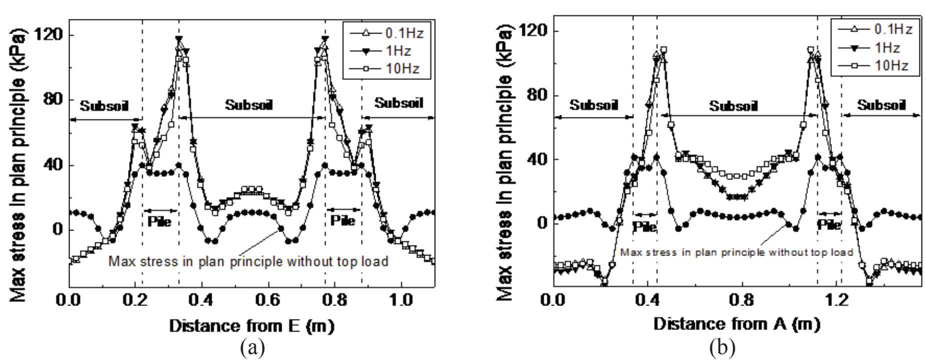

Figure 7. The tensile stresses in geo-synthetica: (a) Stress alone line AC; (b) Stress alone line EF.

of piles alone line EF in Figure 7(b). This is just corresponding to the relationship of load part B% and load frequency.

5 Conclusions

In this study, a 3-D numerical model was built to investigate the arching effect on pile-supported embankment subjected to cyclic loading. Based on the analysis results, the following conclusions can be drawn:

1. Through a comparison between the 3-D numerical analysis and the scale test in terms of settlement and vertical stresses on the top surfaces of pile and subsoil, the reliability of the proposed simulation method was demonstrated.
2. The settlement distribution and development of 0.1 Hz and 1 Hz always has a quit similar regulation but differ from 10 Hz that the displacements under cyclical load of lower frequency 0.1 Hz and 1 Hz increasing faster than the higher one. The settlement caused by cyclic load is much higher than the displacement under static load.
3. The load transfer efficiency of the overall reinforcement is decreased under cyclic load, among which the load part A and B both decreased in different degree. The development of load part A% directly transmitted by the soil arch to pile shows a tiny difference with frequency that decreased with cycles till to be stable, while load part B% through the geo-synthetics to pile is varied with frequency that high-frequency has a lower value than low-frequency.
4. After the local loading, area and value of the maximum tensile stresses is changed a lot that the stress under cyclic load is much higher than those without top load.

References

BS8006-1: 2010. Code of practice for strengthened/reinforced soils and other fills. BritishStandards Institution, ISBN 978-0-580-53842-1.

EBGEO, 2010 (in German). Recommendations for Design and Analysis of Earth Structures Using Geosynthetic Reinforcements-EBGEO[M]. John Wiley & Sons, 2010.

Jones, C.J.F.P., Lawson, C.R., Ayres, D.J., 1990. In: Den Hoedt (Ed.), Geotextile Reinforced Piled

Villard, P., Le Hello, B., Nancey, A., Chew, S.H., Loke, K.H., 2004. Use of high strength geotextiles over piles results from a full scale test. Proc. the 3nd European Geosynthetics Conference, Munich, Germany, vol. 1, pp. 295–298. 01–04 March.

Le Hello B, Villard P. Embankments reinforced by piles and geosynthetics—Numerical and experimental studies dealing with the transfer of load on the soil embankment[J]. Engineering Geology, 2009, 106(1): 78-91.

Low, B.K., Tang, S.K., Choa, V., 1994. Arching in piled embankments. ASCE Journal of Geotechnical Engineering 120, 1917–1938.

Russell, D., Pierpoint, N., 1997. An assessment of design methods for piled embankments. Ground Engineering 39–44 November.

Van Eekelen S J M, Bezuijen A, Lodder H J, et al. Model experiments on piled embankments. Part I[J]. Geotextiles and Geomembranes, 2012, 32: 69-81.

Van Eekelen S J M, Bezuijen A, Lodder H J, et al. Model experiments on piled embankments. Part II[J]. Geotextiles and Geomembranes, 2012, 32: 82-94.

Van Eekelen S J M, Bezuijen A, Van Tol A F. An analytical model for arching in piled embankments[J]. Geotextiles and Geomembranes, 2013, 39: 78-102.

Heitz C, Lüking J, Kempfert H G. Geosynthetic reinforced and pile supported embankments under static and cyclic loading[J]. Strain, 2008, 1: 1-5.

Han J, Bhandari A. Evaluation of geogrid-reinforced pile-supported embankments under cyclic loading using discrete element method[M]//Advances in Ground Improvement: Research to Practice in the United States and China. 2009: 73-82.

Terzaghi, K. (1943). Theoretical soil mechanics, J. Wiley and Sons, New York.